Substantial increase in concurrent droughts and heatwaves in the United States

Omid Mazdiyasni and Amir AghaKouchak[1]

Center for Hydrometeorology and Remote Sensing, Department of Civil and Environmental Engineering, University of California, Irvine, CA 92697

Edited by Benjamin D. Santer, Lawrence Livermore National Laboratory, Livermore, CA, and approved July 31, 2015 (received for review December 3, 2014)

A combination of climate events (e.g., low precipitation and high temperatures) may cause a significant impact on the ecosystem and society, although individual events involved may not be severe extremes themselves. Analyzing historical changes in concurrent climate extremes is critical to preparing for and mitigating the negative effects of climatic change and variability. This study focuses on the changes in concurrences of heatwaves and meteorological droughts from 1960 to 2010. Despite an apparent hiatus in rising temperature and no significant trend in droughts, we show a substantial increase in concurrent droughts and heatwaves across most parts of the United States, and a statistically significant shift in the distribution of concurrent extremes. Although commonly used trend analysis methods do not show any trend in concurrent droughts and heatwaves, a unique statistical approach discussed in this study exhibits a statistically significant change in the distribution of the data.

climate change | drought | heatwave | compound climate extremes | concurrent extremes

Heatwaves cause severe damage to society and the environment (1), with impacts on human health, air quality, and vegetation (2, 3). In 2003, for example, European countries faced an unprecedented heatwave, which in turn caused unusually high ozone concentrations (3) and severe health problems, particularly in France, where 15,000 extra deaths occurred (3–5). United Nations Environment Programme considers the European heatwave the world's most costly weather-related disaster in 2003. Impacts were exacerbated because the region was in a drought (6).

Heatwaves have a variety of direct, indirect, immediate, and delayed impacts, including higher water loss via evapotranspiration, lower yields of grains and other agricultural products (7), increased energy consumption, a decrease in efficiency of power plants (8), air pollution, and adverse effects on human health (3, 6). Heatwaves have also contributed to an increase in the duration, size, and intensity of wildfires, causing economic losses and catastrophic environmental impacts (8).

Droughts also have pronounced impacts on society and the environment, such as significant reductions in gross primary productivity, leading to shortages in food production and increases in global food prices (2). The annual economic damage caused by droughts is estimated to be approximately $7 billion globally (9), with potential impacts on livestock, transportation by river, hydropower production, bioenergy, and energy consumption (8, 10–12).

Extreme climatic events can occur simultaneously, exacerbating environmental and societal impacts. Environmental hazards often result from a combination of climatic events (13, 14) over a range of spatial and temporal scales (15, 16). A wildfire, for example, may occur on a hot, dry, and windy day, although each of these individual conditions may not necessarily be extreme by themselves (16). In the Intergovernmental Panel on Climate Change special report on managing the risks of extreme events and disasters, the combination of multiple climate extreme events is termed a compound event (14, 16). Most analyses of climate and weather extremes typically tend to focus on a single climatic condition; however, this univariate approach may underestimate the effects of concurrent and compound extremes (16).

Sustained precipitation deficit in summer can be a contributory factor to hot summer days (17). Heatwaves reduce the total energy transfer to the atmosphere, resulting in a decrease in convective precipitation (7). This in turn causes a soil–precipitation feedback loop that tends to extend or intensify drought conditions (7). The interaction between precipitation and temperature has been widely recognized in numerous studies (18, 19). Heatwaves concurrent with droughts can intensify individual impacts of heatwaves or drought on society, the environment, and the global economy (19, 20). Studies suggest that changes in the relationship between precipitation and temperature may be more important than the changes in each of the variables individually (16, 21). This study investigates changes in concurrent droughts and heatwaves in the United States using several different statistical techniques.

A heatwave is typically defined as a period of consecutive extremely hot days (22, 23), such as five consecutive days with temperature above the 90th percentile. Here, we use the 85th, 90th, and 95th percentiles of the warm season (May–October) temperature as extreme thresholds, and three heatwave durations (3 d, 5 d, and 7 d). A 5-d heatwave with a 90th percentile threshold is defined as five consecutive days with the maximum temperature exceeding the 90th percentile of the long-term climatology for that month. In this study, meteorological droughts are defined as precipitation deficits relative to the climatology using the Standardized Precipitation Index (SPI) (24). Throughout this study, a drought is defined as an event that leads to SPI < -0.8 (approximately the 20th percentile precipitation). We use daily temperature and monthly precipitation information to identify historical droughts and heatwaves in the United States (see *Data*).

Significance

Climatic extremes cause significant damage to the environment and society, and can cause even more damage when multiple extremes occur simultaneously. This study shows that although there is no significant trend in meteorological drought, the concurrence of meteorological droughts and heatwaves shows statistically significant increases across the United States. We show that the tail of the distribution of concurrent drought and heatwave conditions has shifted toward more frequent and extreme concurrent extremes. Our study outlines a statistical approach for investigating continuous change in the cumulative distribution functions of climatic extremes.

Author contributions: A.A. designed research; O.M. performed research; O.M. analyzed data; and O.M. and A.A. wrote the paper.

The authors declare no conflict of interest.

This article is a PNAS Direct Submission.

Freely available online through the PNAS open access option.

[1]To whom correspondence should be addressed. Email: amir.a@uci.edu.

This article contains supporting information online at www.pnas.org/lookup/suppl/doi:10.1073/pnas.1422945112/-/DCSupplemental.

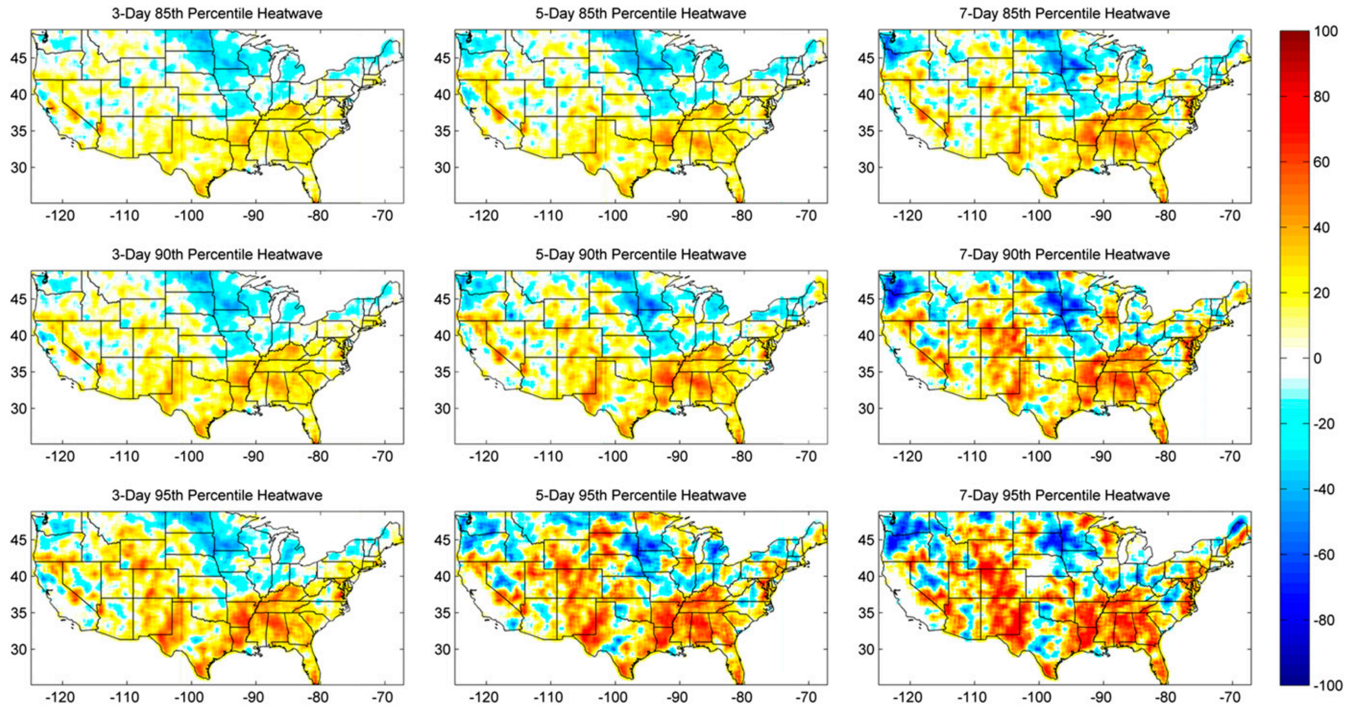

Fig. 1. Percent (%) change in concurrent droughts and heatwaves during 1990–2010 relative to 1960–1980 for each grid box. The rows change in heatwave severity (85th percentile, 90th percentile, and 95th percentile), and the columns change in heatwave duration (3 d, 5 d, and 7 d).

Results

We evaluated the changes in concurrent droughts and heatwaves during 1990–2010 relative to the baseline period 1960–1980. Fig. 1 displays percent change in the occurrences of concurrent drought and heatwave events in each grid box (see also Figs. S1 and S2). Here, the percent change is based on the difference in the number of events in 1990–2010 relative to 1960–1980, divided by the total number of events. We present results for different durations (3-, 5-, and 7-d heatwaves) and extreme temperature thresholds (85th, 90th, and 95th percentiles). Fig. 1 shows that concurrences of all combinations of drought and heatwave intensities and durations have increased substantially in the south, southeast, and parts of the western United States, and have decreased in parts of the Midwest and northern United States. Notably, the longer and more severe (7-d 95th percentile) drought and heatwave concurrences have increased more than shorter, less severe concurrences (e.g., compare 7-d 95th percentile with the 3-d 85th percentile panels). This indicates that longer heatwaves (i.e., 7 d) have become more frequent in 1990–2010 compared with the shorter heatwaves (i.e., 3 d).

Investigating the empirical cumulative distribution function (CDF) of the concurrent droughts and heatwaves reveals a substantial change in extremes in 1990–2010 relative to 1960–1980 (Fig. 2). The x axes represent the percent (%) of the contiguous United States in concurrent drought and heatwave. The y axes show the corresponding cumulative probability. In each panel, the blue line is the CDF for the baseline period and the red line represents the CDF for 1990–2010. The CDF is based on data from the continental United States. As shown, for all intensities and durations during 1990–2010, the upper tail of the CDF has shifted to the right, indicating more extreme events in 1990–2010 relative to the baseline period (compare the red and blue lines in Fig. 2). Notice that the shift is far more pronounced in the more extreme 7-d 95th percentile drought and heatwave concurrence compared with other combinations. The two-sample Kolmogorov–Smirnov (KS) test (*Methods*) confirms that the CDFs of the concurrent droughts and heatwaves in the second period (1990–2010) are substantially different from those in the baseline period (1960–1980) at 0.05 significance level (95% confidence) for all heatwave durations and intensities except for 3-d 85th percentile heatwaves (Table 1).

Past studies focused on changes in drought trends report conflicting results (9, 21, 25, 26). Here, we investigate the percent of the continental United States in concurrent droughts and heatwaves for different durations and intensities from 1960 through 2010 (Fig. 3; see also Fig. S3). For the 90th percentile threshold, the percent of the country in drought and heatwave can range between 6% (7-d heatwave) and 9.6% (3-d heatwave); see the boxplots of the percent contiguous United States (CONUS) in concurrent drought and heatwave for all durations and severities in Fig. S4. Although the CDFs clearly indicate changes in concurrent droughts and heatwaves, the commonly used Mann–Kendall (MK) trend test (see *Methods*) does not show a statistically significant trend (95% confidence) in the fraction of CONUS under concurrent drought and heatwave (Table S1 provides the test statistics results). This can be attributed to limitations of statistical trend tests discussed in previous studies (27) or to lack of sensitive tools for change detection.

Here, we explore an approach based on the Cramér–von Mises change point detection test statistic (see *Methods* and *Supporting Information*) to investigate changes in concurrent droughts and heatwaves. We argue that this method is more sensitive to potential changes in time series and is well suited to investigate climate time series. This method, primarily used in economics and finance, evaluates different periods of data and determines statistically significant changes throughout time series. Fig. 4 shows the Cramér–von Mises statistics for drought and heatwave concurrences during 1960–2010. The y axes indicate a dimensionless measure of divergence between the empirical distributions of data before and after any given year as a continuous function (see *Methods*). For all plots, the maximum divergence occurs between 1998 and 1999, indicating substantial departure of the drought and heatwave CDFs before and after

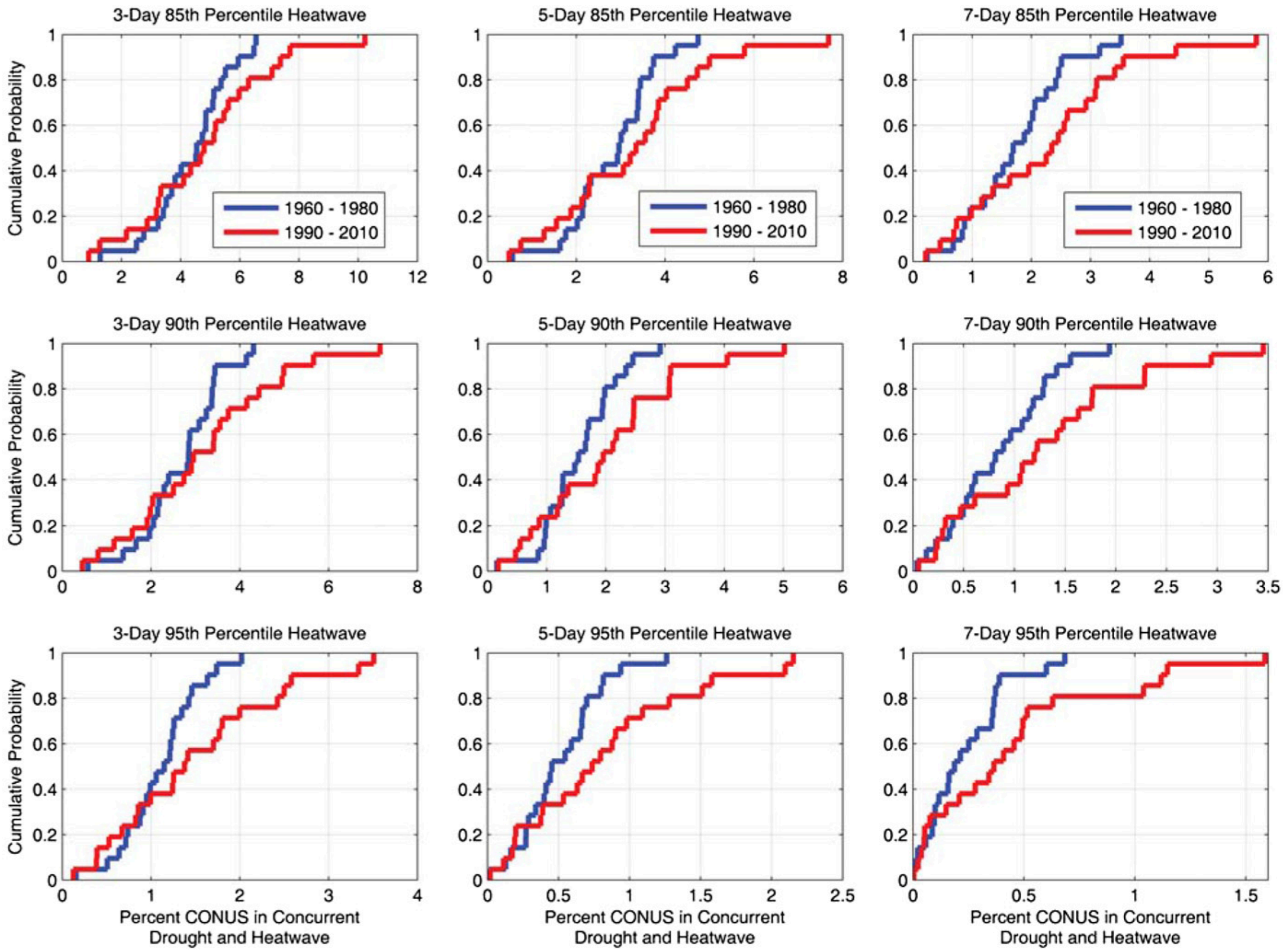

Fig. 2. The empirical CDF of drought and heatwave concurrences from 1960 to 1980 (blue) and 1990 to 2010 (red). The *x* axes represent the percent (%) of CONUS in concurrent drought and heatwave (see *SI Data Sources and Processing* for more information on percent of CONUS). The rows change in heatwave severity (85th percentile, 90th percentile, and 95th percentile), and the columns change in heatwave duration (3 d, 5 d, and 7 d).

the red line in Fig. 4. This information cannot be achieved from the commonly used trend analysis method or distribution change evaluation approaches.

Recent reports suggest an apparent hiatus or so-called pause in global warming since 1999–2000 (28). Possible explanations include a long-lasting solar energy output minimum, low stratospheric water vapor, an increase in early 21st century volcanic activity, and a more frequent La Niña phase since the major El Niño event of 1997–1998 (28). However, analyses show no pause in the occurrence of hot extremes over land since 1997 (29), or even in the mean global temperature (30). Rather, during the hiatus, exceedances of 30 extreme warm days per year have increased (29). The results in Figs. 2 and 4 indicate a statistically significant (at the 0.05 significance level) change in concurrent drought and heatwave events across many regions. Fig. 2 indicates more extreme drought and heatwave concurrences in the latter two decades. This is consistent with the increase in extreme warm days during this period (29). However, this conclusion cannot be reached using the commonly used statistical trend analysis techniques (e.g., MK trend test) used in hydrology and climate literature. Unlike the MK trend test, which investigates monotonic changes in the ranks of variables over time, the Cramér–von Mises test focuses on changes in the distributions of subsamples of the data (Table S2 provides the test statistics results). Typically, climatologists evaluate a certain period against a baseline. The Cramér–von Mises test is a flexible approach that allows investigators to examine different subsamples (e.g., projected and baseline periods) for potential distributional changes. The methodology outlined in this paper shows statistical changes in extremes beyond those achieved with commonly used methods.

Data

Both precipitation and temperature data sets are from the observation-based forcings developed for the North American Land Data Assimilation System Variable Infiltration Capacity simulations over CONUS (31, 32). Daily temperature and monthly precipitation data with a spatial resolution of 1/8° are used for detecting droughts and heatwaves (see *Supporting Information* for more information on the data).

Methods

Here, the two-sample KS test assesses differences between the CDFs of the concurrent drought and heatwave events. KS is a nonparametric test that can evaluate two distribution functions (two-sample) based on the distance between their empirical distribution functions. The null hypothesis is that the two distribution functions are drawn from the same distribution at a certain significance level (here, $\alpha = 0.05$). We use the two-sample KS test to compare different types of droughts and heatwaves (e.g., 3-d 85th percentile, 5-d 90th percentile) in 1990–2010 relative to 1960–1980. The test indicates whether the data from the two periods come from the same distribution at a 0.05 significance level.

Table 1. Change in distribution functions between 1960–1980 and 1990–2010 based on the KS test

Drought and heatwave	*P* value
3-d, 85th percentile	0.53090
5-d, 85th percentile	∼0
7-d, 85th percentile	∼0
3-d, 90th percentile	∼0
5-d, 90th percentile	∼0
7-d, 90th percentile	∼0
3-d, 95th percentile	∼0
5-d, 95th percentile	∼0
7-d, 95th percentile	∼0

Column 2 shows the corresponding *P* values, where *P* values smaller than 0.05 indicate the distribution functions are drawn from different distributions at a 0.05 significance level. Smaller *P* values represent higher confidence in rejecting the null hypothesis that the distributions come from the same distribution.

The MK trend test (33) here assesses the presence of a statistically significant (0.05 significance level) trend in the time series of the fraction of CONUS in concurrent drought and heatwave. The MK test is a nonparametric approach based on the empirical ranks of time series widely used in hydrology and climatology.

We use a framework based on the Cramér–von Mises change point detection to evaluate temporal changes in the concurrent drought and heatwave events (34–37). This approach detects changes in the empirical CDF by comparing two subsamples [$\hat{F}_S(x)$ and $\hat{F}_T(x)$] of the original time series,

$$\hat{F}_S(x) = \frac{1}{\tau}\sum_{i=1}^{\tau} I(X_i \le x)$$

$$\hat{F}_T(x) = \frac{1}{n-\tau}\sum_{i=\tau+1}^{n} I(X_i \le x),$$

where $\hat{F}_S(x)$ and $\hat{F}_T(x)$ are the empirical CDF of the two subsamples, *I* is the indicator function, *n* denotes sample size, and the terms $1/\tau$ and $1/(n - \tau)$ are adjustment factors for the length of each subsample. The test measures the divergence between the empirical distributions as

$$W_{\tau,n} = \int_{-\infty}^{\infty} \left|\hat{F}_S - \hat{F}_T\right|^2 dF_t(x)$$

where $W_{\tau,n}$ can be computed as the square of the mean distance between the empirical distributions (37, 38),

$$W_{\tau,n} = \sum_{i=1}^{n} \left|\hat{F}_S(X_i) - \hat{F}_T(X_i)\right|^2.$$

Larger divergence values, *W*, indicate greater changes in the cumulative distributions. Here, the null hypothesis is that there is no change in the data over time and the two subsamples come from the same distribution. The null hypothesis is rejected if at an unspecified point τ, $\hat{F}_S(x)$ and $\hat{F}_T(x)$ come from statistically different distributions. Because we do not have any prior information on the position of τ in the time series, the test involves computing $W_{\tau,n}$ for all $1 < \tau < n$ (39). However, for different values of τ, the variance of the two subsamples will be different. For this reason, the $W_{\tau,n}$ statistics are adjusted so that both periods exhibit equal mean and variance for all values of τ (39) (see *Supporting Information* for more). The methods in this study

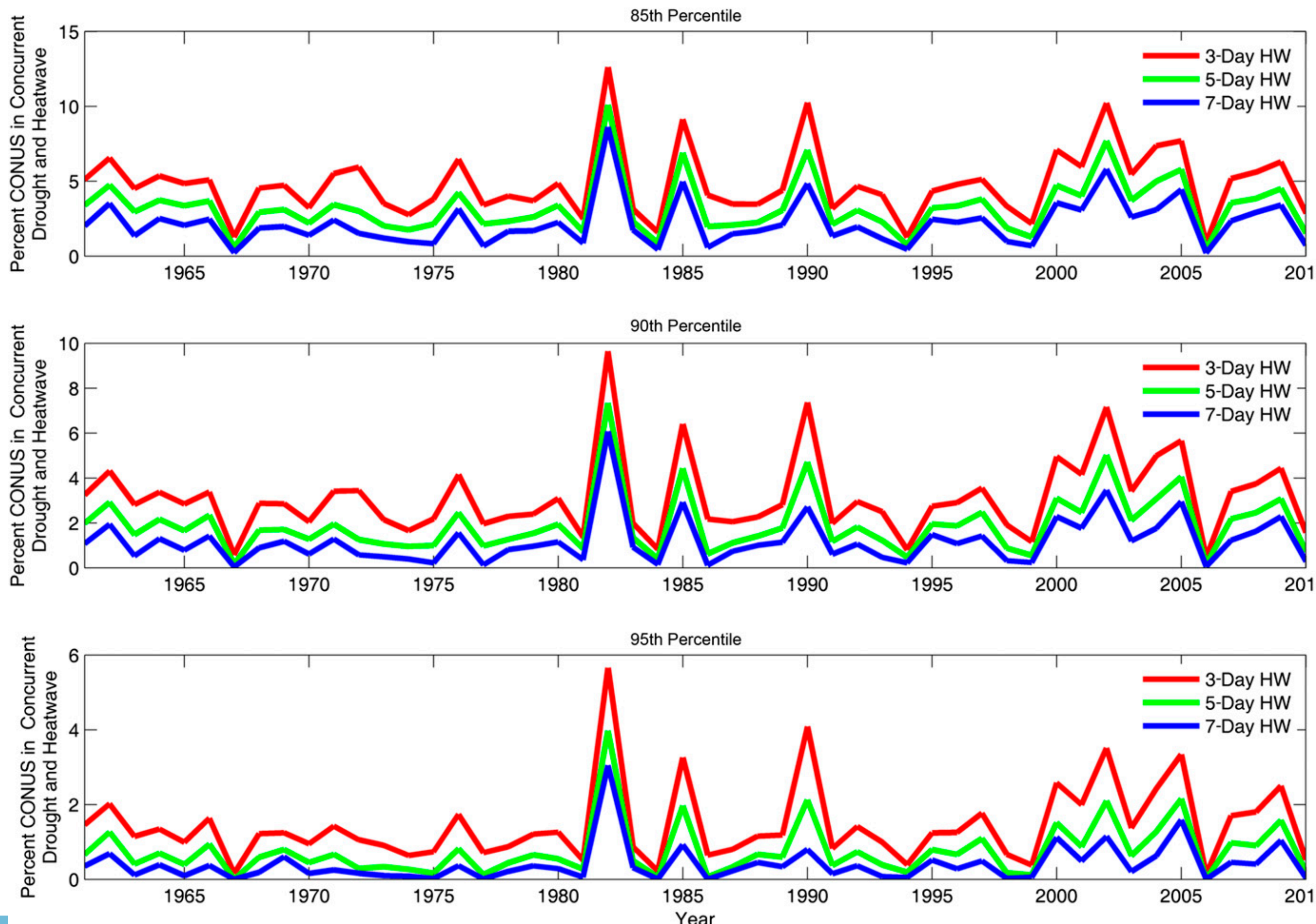

Fig. 3. Percent (%) of CONUS in concurrent drought and heatwave from 1960 to 2010.

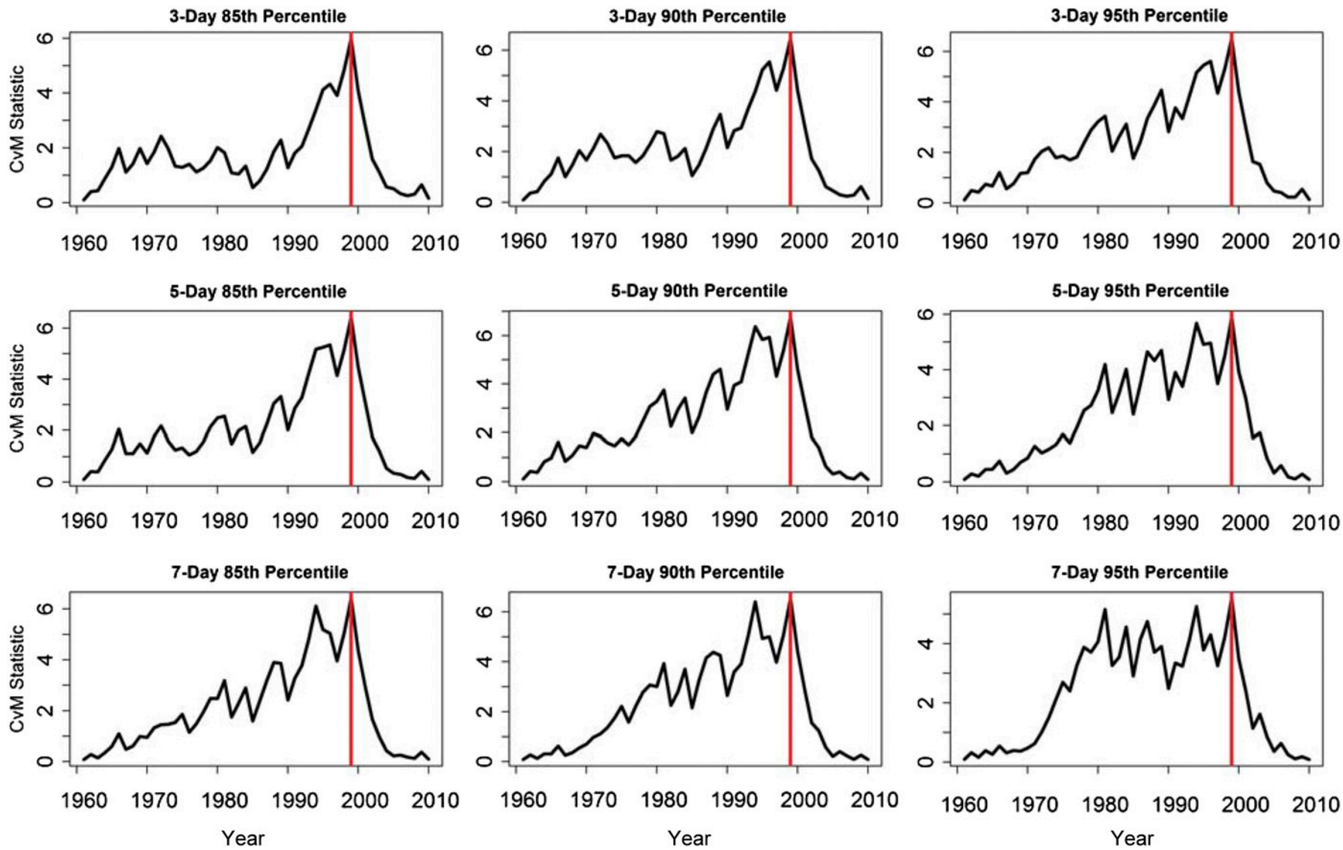

Fig. 4. The Cramér−von Mises (CvM) change point statistic from 1960 to 2010. The rows change in heatwave severity (85th percentile, 90th percentile, and 95th percentile), and the columns change in heatwave duration (3 d, 5 d, and 7 d). The red lines indicate the point of maximum divergence between the distributions of concurrent drought and heatwave events.

should be applied to independent and identically distributed time series. *Supporting Information* provides more information on the sampling approach and temporal autocorrelation of the data (see Fig. S5 and the corresponding discussion).

ACKNOWLEDGMENTS. This study is supported by the National Oceanic and Atmospheric Administration Modeling, Analysis, Prediction, and Projections program Award NA14OAR4310222 and the National Science Foundation Award EAR-1316536.

1. Easterling DR, et al. (2000) Climate extremes: Observations, modeling, and impacts. *Science* 289(5487):2068–2074.
2. Ciais P, et al. (2005) Europe-wide reduction in primary productivity caused by the heat and drought in 2003. *Nature* 437(7058):529–533.
3. Vautard R, et al. (2005) Simulation of ozone during the August 2003 heat wave and emission control scenarios. *Atmos Environ* 39(16):2957–2967.
4. Seneviratne SI, et al. (2012) Changes in climate extremes and their impacts on the natural physical environment. *Managing the Risks of Extreme Events and Disasters to Advance Climate Change Adaptation*, eds Field CB, et al. (Cambridge Univ Press, New York), pp 109−230.
5. Beniston M (2004) The 2003 heat wave in Europe: A shape of things to come? An analysis based on Swiss climatological data and model simulations. *Geophys Res Lett* 31(2):L02202.
6. Poumadère M, Mays C, Le Mer S, Blong R (2005) The 2003 heat wave in France: Dangerous climate change here and now. *Risk Anal* 25(6):1483–1494.
7. Zaitchik BF, et al. (2006) Europe's 2003 heat wave: A satellite view of impacts and land–atmosphere feedbacks. *Int J Climatol* 26(6):743–769.
8. Zamuda C, et al. (2013) *US Energy Sector Vulnerabilities to Climate Change and Extreme Weather* (Dep of Energy, Washington, DC), DOE/PI-0013.
9. Hao Z, et al. (2014) *Global Integrated Drought Monitoring and Prediction System. Scientific Data* 1:140001.
10. Greve P, et al. (2014) Global assessment of trends in wetting and drying over land. *Nat Geosci* 7(10):716–721.
11. Hao Z, AghaKouchak A (2013) Multivariate Standardized Drought Index: A parametric multi-index model. *Adv Water Resour* 57:12–18.
12. Wehner M, et al. (2011) Projections of future drought in the continental United States and Mexico. *J Hydrometeorol* 12(6):1359–1377.
13. AghaKouchak A, Cheng L, Mazdiyasni O, Farahmand A (2014) Global warming and changes in risk of concurrent climate extremes: Insights from the 2014 California drought. *Geophys Res Lett* 41(24):8847–8852.
14. Seneviratne SI, Lüthi D, Litschi M, Schär C (2006) Land-atmosphere coupling and climate change in Europe. *Nature* 443(7108):205–209.
15. Hegerl GC, Hanlon H, Beierkuhnlein C (2011) Climate science: Elusive extremes. *Nat Geosci* 4(3):142–143.
16. Leonard M, et al. (2014) A compound event framework for understanding extreme impacts. *WIREs Clim Change* 5(1):113–128.
17. Mueller B, Seneviratne SI (2012) Hot days induced by precipitation deficits at the global scale. *Proc Natl Acad Sci USA* 109(31):12398–12403.
18. Hao Z, et al. (2013) Changes in concurrent monthly precipitation and temperature extremes. *Environ Res Lett* 8(3):034014.
19. Shukla S, et al. (2015) Temperature impacts on the water year 2014 drought in California. *Geophys Res Lett* 42(11):4384–4393.
20. Perkins SE, Alexander LV, Nairn JR (2012) Increasing frequency, intensity and duration of observed global heatwaves and warm spells. *Geophys Res Lett* 39(20):L20714.
21. Trenberth KE, et al. (2014) Global warming and changes in drought. *Nat Clim Change* 4(1):17–22.
22. Perkins SE, Alexander LV (2013) On the measurement of heat waves. *J Clim* 26(13): 4500–4517.
23. Meehl GA, Tebaldi C (2004) More intense, more frequent, and longer lasting heat waves in the 21st century. *Science* 305(5686):994–997.
24. McKee TB, Doesken NJ, Kleist J (1993) The relationship of drought frequency and duration to time scales. *Proceedings of the 8th Conference on Applied Climatology* (Am Meteorol Soc, Boston) pp 179−184.
25. Sheffield J, Wood EF, Roderick ML (2012) Little change in global drought over the past 60 years. *Nature* 491(7424):435–438.
26. Damberg L, AghaKouchak A (2013) Global trends and patterns of drought from space. *Theor Appl Climatol* 117(3-4):441–448.
27. Clarke RT (2010) On the (mis)use of statistical methods in hydro-climatological research. *Hydrol Sci J* 55(2):139–144.
28. Held IM (2013) Climate science: The cause of the pause. *Nature* 501(7467):318–319.
29. Seneviratne SI, et al. (2014) No pause in the increase of hot temperature extremes. *Nat Clim Change* 4(3):161–163.
30. Karl TR, et al. (2015) Possible artifacts of data biases in the recent global surface warming hiatus. *Science* 348(6242):1469–1472.

31. Maurer EP, Wood AW, Adam JC, Lettenmaier DP, Nijssen B (2002) A long-term hydrologically-based data set of land surface fluxes and states for the conterminous United States. *J Clim* 15(22):3237–3251.
32. Ben Livneh EA, et al. (2013) A long-term hydrologically based dataset of land surface fluxes and states for the conterminous United States: Update and extensions. *J Clim* 26(23):9384–9392.
33. Kendall MG (1975) *Rank Correlation Measures* (Charles Griffin, London).
34. Holmes M, Kojadinovic I, Quessy J-F (2013) Nonparametric tests for change-point detection à la Gombay and Horváth. *J Multivariate Anal* 115:16–32.
35. Bücher A, Kojadinovic I (2013) A dependent multiplier bootstrap for the sequential empirical copula process under strong mixing arxiv:1306.3930, Version 1.
36. Cramér H (1928) On the composition of elementary errors: First paper: Mathematical deductions. *Scand Actuar J* 1928(1):13–74.
37. Sharkey P, Killick R (2014) *Nonparametric Methods for Online Changepoint Detection* (Lancaster Univ, Lancaster, UK).
38. Bücher A, Kojadinovic I (2014) A dependent multiplier bootstrap for the sequential empirical copula process under strong mixing. arxiv:1306.3930, Version 2.
39. Ross GJ, Adams NM (2012) Two nonparametric control charts for detecting arbitrary distribution changes. *J Qual Technol* 44(2):102–116.
40. Shepard DS (1984) Computer mapping: The SYMAP interpolation algorithm. *Spatial Statistics and Models*, eds Gaile GL, Willmott CJ (D. Reidel, Dordrecht, The Netherlands), pp 133–145.
41. Widmann M, Bretherton CS (2000) Validation of mesoscale precipitation in the NCEP reanalysis using a new gridcell dataset for the northwestern United States. *J Clim* 13(11):1936–1950.
42. Ross GJ, Adams NM (2012) Two nonparametric control charts for detecting arbitrary distribution changes. *J Qual Technol* 44(2):102–116.
43. Anderson TW (1962) On the distribution of the two-sample Cramer–von Mises criterion. *Ann Math Stat* 33(3):1148–1159.
44. Hawkins DM, Deng Q (2010) A nonparametric change-point control chart. *J Qual Technol* 42(2):165–173.
45. Gombay E, Horvath L (1999) Change-points and bootstrap. *Environmetrics* 10(6):725–736.
46. Bücher A, Kojadinovic I, Rohmer T, Segers J (2014) Detecting changes in cross-sectional dependence in multivariate time series. *J Multivar Anal* 132:111–128.
47. Politis DN, Halbert W (2004) Automatic block-length selection for the dependent bootstrap. *Econom Rev* 23(1):53–70.
48. Anderson TW, Darling DA (1952) Asymptotic theory of certain "goodness of fit" criteria based on stochastic processes. *Ann Math Stat* 23:193–212.